Differential polarization imaging
IV. Images in higher Born approximations

Myeonghee Kim and Carlos Bustamante
Department of Chemistry, The University of New Mexico, Albuquerque, New Mexico 87131 USA

ABSTRACT The theory of differential polarization imaging developed previously within the framework of the first Born approximation is extended to higher Born approximations, taking into account interactions among the polarizable groups in the object. Several properties of differential polarization images, originally described using first Born approximation are modified when higher Born approximations are used. In particular, (*a*) when the polarizable groups are spherically symmetric, the off-diagonal Mueller elements M_{ij} ($i \neq j$) in bright field do not vanish in higher Born approximations, as they do in the first Born approximation case. (*b*) In higher Born approximations, the dark field M_{i4} and M_{4i} ($i = 1, 2, 3$) images do not vanish as in the first Born approximation, due to the anisotropy induced by the interactions among the groups. (c) When the polarizability tensor of each group is symmetric and real, the bright field M_{14} and M_{41} images always vanish in the first Born approximation. In higher Born approximations, these terms do not vanish if the groups bear a chiral relationship to each other.

Quantitative criteria for the validity of the first Born approximation in differential polarization imaging are explicitly derived for three different types of media: (*a*) linearly anisotropic, (*b*) circularly anisotropic, and (c) linearly and circularly anisotropic (medium displaying linear birefringence and circular birefringence). These criteria define the limits of thickness and the degree of anisotropy of optically thin media.

Finally, the possibility to perform optical sectioning in differential polarization imaging in the presence and absence of group interactions is discussed.

I. INTRODUCTION

In the first paper of this series (1) (hereafter referred to as paper I), a theory of differential polarization imaging was developed within the framework of the first Born approximation, where the internal field experienced by the polarizable groups is approximated by the incident electric field. This approximation excludes multiple scattering effects and dipole–dipole coupling among the groups in the molecule. The first Born approximation is valid when the density of polarizable groups is relatively low, and the average distance between groups is sufficiently large; in this case the groups react independently to the incident field. On the other hand, if the density of polarizable groups is high, multiple scattering and dipole–dipole coupling occur among the groups and each polarizable group experiences an internal field that is a superposition of the incident field and the fields generated at every other dipole induced in the molecule. This internal field can be described using higher Born approximations.

In this paper, we extend the previous theory of differential polarization imaging to include internal field effects. In section II the fields scattered and transmitted by an object are obtained in the nth Born approximation. These fields are then transformed by a thin lens within the paraxial approximation to obtain their amplitude on a detector screen in the dark and bright field imaging geometries. The equations are then generalized for the exact case (infinite Born approximation). This section concludes with an analysis of how differential polarization images are modified by the mutual interactions among the polarizable groups. Section III discusses in detail the effect of higher Born approximations on the optical activity images of chiral objects. This analysis is done in bright and dark field imaging. In section IV, criteria for the validity of the first Born approximation in differential polarization imaging are derived for three different types of optical media. Section V discusses the feasibility of performing optical sectioning in bright field differential polarization imaging of optically dense objects.

Address correspondence to Dr. Carlos Bustamante.
Dr. Bustamante's present address is Institute of Molecular Biology, University of Oregon, Eugene, OR 97403.

II. FIELDS IN HIGHER BORN APPROXIMATIONS

The electric field equation on a detector screen in dark field imaging geometry is (see paper I [1]):

$$\mathbf{E}_{sct,D}(\mathbf{r}) = D'(2\hat{\mathbf{r}} - \hat{\mathbf{r}} \cdot \hat{\mathbf{z}}) \cdot \sum_i e^{-ik\hat{\mathbf{z}}\cdot\mathbf{r}_i} K_i \boldsymbol{\alpha}_i \cdot E_o e^{ik_o \cdot r_i} \hat{\boldsymbol{\epsilon}}_o, \quad (1)$$

0006-3495/91/06/1171/12 $2.00

where $\mathbf{r}$ is a vector pointing from the center of the lens to an image point on the detector screen, and $\hat{\mathbf{z}}$ is a unit vector along the z direction. The z-axis is the optical axis along which the sample, the lens, and the detector screen are aligned. $\mathbf{k}_o = 2\pi/\lambda\ \hat{\mathbf{k}}_o = k\hat{\mathbf{k}}_o$, where λ is the wavelength of the incident light, and $\hat{\mathbf{k}}_o$ is the unit vector in the direction along which the incident light propagates. $\mathbf{r}_i$ and α_i are the position vector and the polarizability tensor of the ith polarizable group in the object, respectively. E_o and $\hat{\epsilon}_o$ are the amplitude and polarization unit vector of the incident electric field, respectively.

$$D' = \frac{iPk^3a^2}{rr_o} e^{ik(r+r_o+n\Delta_o+\hat{k}_o\cdot x_o)},$$

where P is a constant that depends on the transmittance of the lens material and on the thickness of the lens. a, n, and Δ_o are the radius, the refractive index, and the thickness of the lens at its center, respectively. $r = |\mathbf{r}|$, $r_o = |\mathbf{x}_o|$, and $\mathbf{x}_o$ is the vector pointing from the center of the lens to the origin of coordinates in the object (refer to Fig. 1 of paper I for more detailed notations [1]).

$$K_i = \frac{J_1\left(\frac{ka\rho_i}{r}\right)}{\frac{ka\rho_i}{r}},$$

where

$$J_1\left(\frac{ka\rho_i}{r}\right)$$

is a Bessel function of the first kind of order one and

$$\rho_i = \sqrt{(x + mx_i)^2 + (y + my_i)^2}.$$

x and y are the Cartesian coordinates of $\mathbf{r}$, x_i and y_i are cartesian coordinates of $\mathbf{r}_i$; and m is the magnification of the imaging system. K_i is a function which describes the diffraction patterns of a collection of oscillating point dipoles inside an object. In the first Born approximation, the ith oscillating dipole moment is given by:

$$\boldsymbol{\mu}_i = \alpha_i \cdot E_o e^{i\mathbf{k}_o\cdot\mathbf{r}_i}\hat{\epsilon}_o,$$

where the oscillating dipole moment is described by the internal product between the polarizability tensor α_i, describing the point polarizable group located at $\mathbf{r}_i$, and the incident electric field $E_o e^{i\mathbf{k}_o\cdot\mathbf{r}_i}\hat{\epsilon}_o$ at $\mathbf{r}_i$. In other words, the internal electric field at $\mathbf{r}_i$ is approximated by the incident field. However, if groups are close together, each polarizable group feels the superposition of the incident field and the secondary waves from all other dipoles induced in neighboring groups. In higher Born approximations, the effects of the secondary waves are included in the expression of the internal field.

To obtain an expression of $\mathbf{E}_{scr,D}(\mathbf{r})$ in higher Born approximations, first we must find an adequate expression to the internal field, $\mathbf{E}_{internal}$ at $\mathbf{r}_i$. In the theory of polarized light scattering, this result has been obtained by McClain et al. (2) and by Bustamante et al. (3). For a review on higher Born effects in circularly polarized light scattering, see Tinoco et al. (4). The internal field at $\mathbf{r}_i$ can be written:

$$\mathbf{E}_{internal}(\mathbf{r}_i) = \mathbf{E}_o(\mathbf{r}_i) + \mathbf{E}_{induced}(\mathbf{r}_i), \tag{2}$$

where $\mathbf{E}_{induced}(\mathbf{r}_i)$ is the superposition of the fields due to the dipole moments induced at all other groups in the molecule. In the first Born approximation, $\mathbf{E}_{induced}$ is neglected relative to $\mathbf{E}_o$. This approximation is valid only when the polarizabilities are weak and the dipoles are far apart so that each dipole may be considered independent of the others. In higher Born approximations, the induced field at $\mathbf{r}_i$ is (5):

$$\mathbf{E}_{induced}(\mathbf{r}_i) = 4\pi k^2 \sum_{j\neq i}^{N} \Gamma_{ij} \cdot \alpha_j \cdot \mathbf{E}_{internal}(\mathbf{r}_j), \tag{3}$$

where Γ_{ij} is the Green's function expressing the coupling between groups i and j in the object, and given explicitly by (5–7)

$$\Gamma_{ij} = (\mathbf{1} - \hat{\mathbf{r}}_{ij}\hat{\mathbf{r}}_{ij})\frac{e^{ikr_{ij}}}{4\pi r_{ij}} + (3\hat{\mathbf{r}}_{ij}\hat{\mathbf{r}}_{ij} - \mathbf{1})\left(\frac{1}{k^2r_{ij}^2} - \frac{i}{kr_{ij}}\right)\frac{e^{ikr_{ij}}}{4\pi r_{ij}} - \frac{\mathbf{1}}{3k^2}\delta^3(\mathbf{r}_{ij}). \tag{4}$$

Here, $r_{ij} = |\mathbf{r}_j - \mathbf{r}_i|$ and $\hat{\mathbf{r}}_{ij} = \mathbf{r}_j - \mathbf{r}_i/r_{ij}$. In the second Born approximation, $\mathbf{E}_{internal}$ in Eq. 3 is approximated by the incident electric field $\mathbf{E}_o(\mathbf{r}_j)$. In the third Born approximation, $\mathbf{E}_{internal}(\mathbf{r}_j)$ in Eq. 3 is again written as:

$$\mathbf{E}_{internal}(\mathbf{r}_j) = \mathbf{E}_o(\mathbf{r}_j) + 4\pi k^2 \sum_{k\neq j}^{N} \Gamma_{jk} \cdot \alpha_k \cdot \mathbf{E}_o(\mathbf{r}_k).$$

Using Eqs. 2 and 3, $\mathbf{E}_{scr,D}(\mathbf{r})$ in the second Born approximation is given by:

$$\mathbf{E}_{scr,D}(\mathbf{r}) = D'(\hat{\mathbf{z}}\hat{\mathbf{r}} - \hat{\mathbf{r}}\cdot\hat{\mathbf{z}}) \cdot \sum_i e^{-ik\hat{\mathbf{r}}\cdot\mathbf{r}_i} \frac{J_1\left(\frac{ka\rho_i}{r}\right)}{\frac{ka\rho_i}{r}} \cdot \left[\alpha_i \cdot \left(\mathbf{1} + 4\pi k^2 \sum_{j\neq i}^{N} \Gamma_{ij} \cdot \alpha_j e^{i\mathbf{k}_o\cdot(\mathbf{r}_j - \mathbf{r}_i)}\right)\right] \cdot E_o e^{i\mathbf{k}_o\cdot\mathbf{r}_i}\hat{\epsilon}_o. \tag{5}$$

Notice that the ith polarizability tensor α_i in Eq. 1 is replaced by the expression in the square brackets in Eq.

5. These terms can be interpreted as the polarizability of the ith group "in the presence of all other groups" inside the particle. They are, therefore, "effective polarizabilities." When groups are close together the dominant interaction is a short-ranged, dipole–dipole coupling described by

$$(3\hat{\mathbf{r}}_{ij}\hat{\mathbf{r}}_{ij} - \mathbf{1})\frac{e^{ikr_{ij}}}{4\pi k^2 r_{ij}^3}$$

(see Eq. 4). When groups are far apart, the radiation coupling term,

$$(\mathbf{1} - \hat{\mathbf{r}}_{ij}\hat{\mathbf{r}}_{ij})\frac{e^{ikr_{ij}}}{4\pi r_{ij}},$$

describing multiple scattering events among the groups inside the medium becomes important. Rearranging Eq. 5, we obtain:

$$\mathbf{E}_{scr,D}(\mathbf{r}) = D''[\hat{\mathbf{z}}\hat{\mathbf{r}} - (\hat{\mathbf{r}}\cdot\hat{\mathbf{z}})\mathbf{1}]\cdot\sum_i e^{-i\Delta\mathbf{k}'\cdot\mathbf{r}_i}\frac{J_1\left(\frac{ka\rho_i}{r}\right)}{\frac{ka\rho_i}{r}}\cdot\left[\alpha_i\cdot\left(\mathbf{1} + 4\pi k^2\sum_{j\neq i}^{N}\Gamma_{ij}\cdot\alpha_j e^{ik_o\cdot r_{ij}}\right)\right]\cdot\hat{\boldsymbol{\epsilon}}_o, \quad (6)$$

where $D'' = E_o D'$ and $\Delta\mathbf{k}' = k(\hat{\mathbf{z}} - \hat{\mathbf{k}}_o)$ is the momentum transfer vector of the light.

In higher Born approximations, $\mathbf{E}_{scr,D}(\mathbf{r})$ remains in the form of Eq. 6, but the definition of the effective polarizability α_i' changes; the effective polarizabilities obey the recursion relation (5),

$$\alpha_i'^{(n+1)} = \alpha_i'^{(n)}\cdot\left(\mathbf{1} + 4\pi k^2\sum_{j=1}^{N}\Gamma_{ij}\cdot\alpha_j'^{(n)}e^{ik_o\cdot r_{ij}}\right), \quad (7)$$

where the polarizabilities $\alpha_j'^{(n)}$ and $\alpha_i'^{(n+1)}$ are effective polarizabilities in the nth or $(n+1)$th Born approximation, respectively. The electric field on a detector screen in the $(n+1)$th Born approximation is obtained replacing α_i appearing in Eq. 1 by the effective polarizability $\alpha_i'^{(n+1)}$.

In the exact case, where no approximations on the internal electric field are made, the ith induced dipole moment $\boldsymbol{\mu}_i$ may be written (6)

$$\boldsymbol{\mu}_i = \sum_{j=1}^{N}\mathbf{A}_{ij}(\hat{\mathbf{t}}_j^*\cdot E_o e^{ik_o\cdot r_j}\hat{\boldsymbol{\epsilon}}_o)\cdot\hat{\mathbf{t}}_i, \quad (8)$$

where $\hat{\mathbf{t}}_i$ is a unit vector describing the directional property of the ith polarizability $\boldsymbol{\alpha}_i$ such that

$$\boldsymbol{\alpha}_i = \alpha_i\hat{\mathbf{t}}_i\hat{\mathbf{t}}_i,$$

and α_i is the magnitude of the ith polarizability. $\mathbf{A}_{ij}$ is the ijth 3×3 block of a matrix whose inverse matrix $\mathbf{A}^{-1}$ is defined by (6)

$$\mathbf{A}^{-1} = \begin{bmatrix} \boldsymbol{\alpha}_1^{-1} & -4\pi k^2\Gamma_{12} & -4\pi k^2\Gamma_{13} & \cdot & \cdot \\ -4\pi k^2\Gamma_{21} & \boldsymbol{\alpha}_2^{-1} & -4\pi k^2\Gamma_{23} & \cdot & \cdot \\ -4\pi k^2\Gamma_{31} & -4\pi k^2\Gamma_{32} & \boldsymbol{\alpha}_3^{-1} & \cdot & \cdot \\ \cdot & \cdot & \cdot & \cdot & \cdot \\ \cdot & \cdot & \cdot & \cdot & \cdot \\ \cdot & \cdot & \cdot & \cdot & \cdot \end{bmatrix}.$$

Replacing $\boldsymbol{\alpha}_i\cdot\mathbf{E}_o(\mathbf{r}_i)$ in Eq. 1 by $\boldsymbol{\mu}_i$ in Eq. 8, we obtain

$$\mathbf{E}_{scr,D}(\mathbf{r}) = D''[\hat{\mathbf{z}}\hat{\mathbf{r}} - (\hat{\mathbf{r}}\cdot\hat{\mathbf{z}})\mathbf{1}]\cdot\left[\sum_i\sum_j\frac{J_1\left(\frac{ka\rho_i}{r}\right)}{\frac{ka\rho_i}{r}}\mathbf{A}_{ij}\cdot\hat{\mathbf{t}}_i\hat{\mathbf{t}}_j^*\right]\cdot\hat{\boldsymbol{\epsilon}}_o. \quad (9)$$

In bright field imaging geometry, the electric field on a detector screen in the first Born approximation is given by (see Eq. 29 in paper I [1]):

$$\mathbf{E}_{scr,B}(\mathbf{r}) = D''[\hat{\mathbf{z}}\hat{\mathbf{r}} - (\hat{\mathbf{r}}\cdot\hat{\mathbf{z}})\mathbf{1}]\cdot\mathbf{G}\cdot\hat{\boldsymbol{\epsilon}}_o, \quad (10)$$

where

$$\mathbf{G} = \frac{r_o^2}{ia^2k^3}\mathbf{1} + \sum_i\frac{J_1\left(\frac{ka\rho_i}{r}\right)}{\frac{ka\rho_i}{r}}\boldsymbol{\alpha}_i.$$

Whereas in the exact case,

$$\mathbf{E}_{scr,B}(\mathbf{r}) = D''[\hat{\mathbf{z}}\hat{\mathbf{r}} - (\hat{\mathbf{r}}\cdot\hat{\mathbf{z}})\mathbf{1}]\cdot\left[\frac{r_o^2}{ia^2k^3}\mathbf{1} + \sum_i\sum_j\frac{J_1\left(\frac{ka\rho_i}{r}\right)}{\frac{ka\rho_i}{r}}\mathbf{A}_{ij}\cdot\hat{\mathbf{t}}_i\hat{\mathbf{t}}_j^*\right]\cdot\hat{\boldsymbol{\epsilon}}_o. \quad (11)$$

Comparing Eq. 10 and 11, it is seen that the expression inside the square brackets in Eq. 11 corresponds to the tensor $\mathbf{G}$ in Eq. 10 with α_i in Eq. 10 replaced by $\mathbf{A}_{ij}\cdot\hat{\mathbf{t}}_i\hat{\mathbf{t}}_j^*$ in Eq. 11. Eqs. 9 and 11 are the expressions required to extend the differential polarization imaging theory to all order interactions (exact case).

Symmetric and real polarizability tensors represent transparent (nonabsorbing) linearly anisotropic groups. However, even if the polarizability tensor $\boldsymbol{\alpha}_i$ is symmetric and real, the effective polarizability tensor in Eq. 7 is neither symmetric nor real due to the terms describing the interactions among the induced dipoles. As a result, several properties of differential polarization images are altered in higher Born approximations. These will be considered next.

II A. Bright field images in higher Born approximations

Bright field Mueller images in higher Born approximations will be compared here with those obtained in the first Born approximation. Two cases are considered: (*a*) the polarizability tensor of the individual groups is isotropic and real. Isotropic tensors with real elements represent groups that neither absorb nor modify the polarization state of the incident light. This type of tensor takes the form of a unit matrix multiplied by a real constant. (*b*) The polarizability tensor is symmetric and its nine elements are real. This type of tensors insures that the groups are nonabsorbing and linearly anisotropic.

In case *a*, all off-diagonal bright field Mueller images (M_{ij} [i ≠ j]) vanish in the first Born approximation. To illustrate this we write the bright field M_{23} with $\boldsymbol{\alpha}_i = \alpha_i \mathbf{1}$[1]:

$$M_{23} \propto [\mathbf{G} \cdot (\hat{\boldsymbol{\epsilon}}^{H}\hat{\boldsymbol{\epsilon}}^{H} - \hat{\boldsymbol{\epsilon}}^{V}\hat{\boldsymbol{\epsilon}}^{V}) \cdot \mathbf{G}]_{\alpha\beta} \cdot (\hat{\boldsymbol{\epsilon}}_{H\alpha}\hat{\boldsymbol{\epsilon}}_{V\beta} + \hat{\boldsymbol{\epsilon}}_{V\alpha}\hat{\boldsymbol{\epsilon}}_{H\beta}) = \left(B^2 + \sum_{i}^{N}\sum_{j}^{N} K_i K_j \alpha_i \alpha_j\right) \cdot [\mathbf{1} \cdot (\hat{\boldsymbol{\epsilon}}^{H}\hat{\boldsymbol{\epsilon}}^{H} - \hat{\boldsymbol{\epsilon}}^{V}\hat{\boldsymbol{\epsilon}}^{V}) \cdot \mathbf{1}]_{\alpha\beta} (\hat{\boldsymbol{\epsilon}}_{H\alpha}\hat{\boldsymbol{\epsilon}}_{V\beta} + \hat{\boldsymbol{\epsilon}}_{V\alpha}\hat{\boldsymbol{\epsilon}}_{H\beta}), \quad (12)$$

where

$$B = \frac{r_o^2}{a^2 k^3}$$

and, as in paper I (1), the subscripts indicate the nature of the incident polarization, horizontal (H) or vertical (V), and the superscripts indicate the polarization component of the light transmitted by the object which is selected by an analyzer placed in front of the photodetector.

This term vanishes because:

$$[\mathbf{1} \cdot (\hat{\boldsymbol{\epsilon}}^{H}\hat{\boldsymbol{\epsilon}}^{H} - \hat{\boldsymbol{\epsilon}}^{V}\hat{\boldsymbol{\epsilon}}^{V}) \cdot \mathbf{1}]_{\alpha\beta} (\hat{\boldsymbol{\epsilon}}_{H\alpha}\hat{\boldsymbol{\epsilon}}_{V\beta} + \hat{\boldsymbol{\epsilon}}_{V\alpha}\hat{\boldsymbol{\epsilon}}_{H\beta}) = (\hat{\boldsymbol{\epsilon}}_{H} \cdot \hat{\boldsymbol{\epsilon}}^{H})(\hat{\boldsymbol{\epsilon}}^{H} \cdot \hat{\boldsymbol{\epsilon}}_{V}) - (\hat{\boldsymbol{\epsilon}}_{H} \cdot \hat{\boldsymbol{\epsilon}}^{V})(\hat{\boldsymbol{\epsilon}}^{V} \cdot \hat{\boldsymbol{\epsilon}}_{V}) + (\hat{\boldsymbol{\epsilon}}_{V} \cdot \hat{\boldsymbol{\epsilon}}^{H})(\hat{\boldsymbol{\epsilon}}^{H} \cdot \hat{\boldsymbol{\epsilon}}_{H}) - (\hat{\boldsymbol{\epsilon}}_{V} \cdot \hat{\boldsymbol{\epsilon}}^{V})(\hat{\boldsymbol{\epsilon}}^{V} \cdot \hat{\boldsymbol{\epsilon}}_{H}) = 0,$$

where we have used the relations, $\hat{\boldsymbol{\epsilon}}_{H} = \hat{\boldsymbol{\epsilon}}^{H}$, $\hat{\boldsymbol{\epsilon}}_{V} = \hat{\boldsymbol{\epsilon}}^{V}$, and $\hat{\boldsymbol{\epsilon}}_{H} \perp \boldsymbol{\epsilon}_{V}$. In higher Born approximations, however, M_{23} is:

$$M_{23} \propto \left(iB \sum_{i}^{N} K_i [(\hat{\boldsymbol{\epsilon}}^{H}\hat{\boldsymbol{\epsilon}}^{H} - \hat{\boldsymbol{\epsilon}}^{V}\hat{\boldsymbol{\epsilon}}^{V}) \cdot \boldsymbol{\alpha}_i' - \boldsymbol{\alpha}_i'^{\dagger} \cdot (\hat{\boldsymbol{\epsilon}}^{H}\hat{\boldsymbol{\epsilon}}^{H} - \hat{\boldsymbol{\epsilon}}^{V}\hat{\boldsymbol{\epsilon}}^{V})] + \sum_{i}^{N}\sum_{j}^{N} K_i K_j \boldsymbol{\alpha}_i'^{\dagger} \cdot (\hat{\boldsymbol{\epsilon}}^{H}\hat{\boldsymbol{\epsilon}}^{H} - \hat{\boldsymbol{\epsilon}}^{V}\hat{\boldsymbol{\epsilon}}^{V}) \cdot \boldsymbol{\alpha}_j'\right)_{\alpha\beta} \cdot (\hat{\boldsymbol{\epsilon}}_{H\alpha}\hat{\boldsymbol{\epsilon}}_{V\beta} + \hat{\boldsymbol{\epsilon}}_{V\alpha}\hat{\boldsymbol{\epsilon}}_{H\beta}),$$

where $\boldsymbol{\alpha}'$ is the effective polarizability tensor given by Eq. 7 and $K_i = J_1(ka\rho_i/r)/(ka\rho_i/r)$ as before. As mentioned previously, this polarizability is neither symmetric nor real.

The term proportional to *iB* is the differential extinction term; using the relations $\hat{\boldsymbol{\epsilon}}_{H} = \hat{\boldsymbol{\epsilon}}^{H} = \hat{\mathbf{x}}$ and $\hat{\boldsymbol{\epsilon}}_{V} = \hat{\boldsymbol{\epsilon}}^{V} = \hat{\mathbf{y}}$, this term becomes

$$iB \sum_{i}^{N} K_i [\hat{\mathbf{x}} \cdot (\boldsymbol{\alpha}_i' + \boldsymbol{\alpha}_i'^{\dagger}) \cdot \hat{\mathbf{y}} - \hat{\mathbf{y}} \cdot (\boldsymbol{\alpha}_i' + \boldsymbol{\alpha}_i'^{\dagger}) \cdot \hat{\mathbf{x}}].$$

The quantity $\boldsymbol{\alpha}_i' + \boldsymbol{\alpha}_i'^{\dagger}$ in the above expression is a symmetric tensor in the second Born approximation, when the zero-order polarizability tensors are real and isotropic. Therefore, this expression vanishes. In the third or higher Born approximations, however, the tensors $\boldsymbol{\alpha}_i' + \boldsymbol{\alpha}_i'^{\dagger}$ are no longer symmetric nor real and the expression does not vanish. Its value depends on the geometrical relationship among the isotropic groups.

The term proportional to $K_i K_j$ describes the forward differential scattering contribution to the image and it does not vanish in the second or in higher Born approximations. This is because the complex phase factors introduced by the interactions among the groups allow the waves scattered in the forward direction to interfere with each other, reflecting the geometrical relationships among the groups.

In case *b*, where polarizability tensor of each group is symmetric and real, most bright field Mueller images survive in the first Born approximation, except the M_{14} and M_{41} images which are always zero, regardless of the geometrical relationship among the groups (see paper I [1]). In higher Born approximations, however, M_{14} and M_{41} do not vanish if the group polarizations maintain a chiral relationship with each other. In the theory of polarized light scattering this effect was first described by McClain et al. (2) and independently by Bustamante et al. (3) (see also Tinoco et al. [4]). This result will be analyzed in more detail in section III A where the effect of group coupling on the imaging of optical activity will be discussed.

II B. Dark field images in higher Born approximations

In dark field imaging, when the group polarizabilities are isotropic and real, the M_{i4} (i = 1, 2, 3) images and their transposes (M_{4i}) vanish. However, when group coupling occurs, these images no longer vanish due to the nonreal and nonsymmetric character of the effective polarizability tensors. This is elaborated in detail for the M_{14} image in section III B.

III. EFFECTS OF COUPLING ON OPTICAL ACTIVITY IMAGES

III A. Bright field M_{14} and M_{41} images of chiral objects by differential removal of right and left circularly polarized incident light

In bright field, both M_{14} and M_{41} are sensitive to optical activity. As mentioned before, M_{14} and M_{41} vanish in the first Born approximation when the polarizability tensors of the groups are symmetric and real. In this section we will show that, in higher Born approximations, groups arranged in a chiral fashion give rise to optical activity effects in the images, even when they are represented by symmetric and real polarizability tensors.

In bright field, M_{14} and M_{41} are (see Eq. 31 in paper I [1]):

$$M_{14} = iA\,(\mathbf{G} \times \mathbf{G}^{\dagger})_{\alpha\beta\gamma}(1 - \hat{\mathbf{z}}\hat{\mathbf{z}})_{\alpha\gamma}\hat{\mathbf{z}}_{\beta}$$
$$M_{41} = iA\,(\mathbf{G}^{\dagger} \times \mathbf{G})_{\alpha\beta\gamma}(1 - \hat{\mathbf{z}}\hat{\mathbf{z}})_{\alpha\gamma}\hat{\mathbf{z}}_{\beta},$$

where we have made the approximation $\hat{\mathbf{r}} \approx \hat{\mathbf{z}}$. Using the expression of the tensor $\mathbf{G}$ in Eq. 10, the above equations can be rewritten:

$$M_{14} = -iA\,[B^2(\mathbf{1} \times \mathbf{1})_{\alpha\beta\gamma} - iB\,(\mathbf{1} \times \mathbf{F}^{\dagger} - \mathbf{F} \times \mathbf{1})_{\alpha\beta\gamma} + (\mathbf{F} \times \mathbf{F}^{\dagger})_{\alpha\beta\gamma}](1 - \hat{\mathbf{z}}\hat{\mathbf{z}})_{\alpha\gamma}\hat{\mathbf{z}}_{\beta} \quad (13)$$

$$M_{41} = -iA\,[B^2(\mathbf{1} \times \mathbf{1})_{\alpha\beta\gamma} + iB\,(\mathbf{1} \times \mathbf{F} - \mathbf{F}^{\dagger} \times \mathbf{1})_{\alpha\beta\gamma} + (\mathbf{F}^{\dagger} \times \mathbf{F})_{\alpha\beta\gamma}](1 - \hat{\mathbf{z}}\hat{\mathbf{z}})_{\alpha\gamma}\hat{\mathbf{z}}_{\beta}. \quad (14)$$

The first group of terms, proportional to B^2, vanishes both in first and higher Born approximations. The second group of terms containing the expressions $(\mathbf{1} \times \mathbf{F}^{\dagger} - \mathbf{F} \times \mathbf{1})_{\alpha\beta\gamma}$ in M_{14} and $(\mathbf{1} \times \mathbf{F} - \mathbf{F}^{\dagger} \times \mathbf{1})_{\alpha\beta\gamma}$ in M_{41}, includes terms which account for the differential extinction: differential absorption (CD) and differential scattering away from the forward direction. These terms vanish in the first Born approximation when the polarizability tensors of the individual groups are symmetric and real. The third group of terms, containing the expressions $(\mathbf{F} \times \mathbf{F}^{\dagger})_{\alpha\beta\gamma}$ in M_{14} and $(\mathbf{F}^{\dagger} \times \mathbf{F})_{\alpha\beta\gamma}$ in M_{41}, accounts for the circular intensity differential scattering (CIDS) in the forward direction, and vanishes in the first Born approximation, when the polarizability tensors of the individual groups are symmetric and real. In higher Born approximations, however, the second and the third groups of terms in M_{14} and M_{41} do not vanish, because the effective polarizability tensors contained in $\mathbf{F}$ are complex and not symmetric, due to the interaction among groups. In particular, the $(\mathbf{F} \times \mathbf{F})_{\alpha\beta\gamma}$ terms survive because the scattered waves can interfere in the forward direction due to the complex phase factors added to the secondary waves by the group interactions. However, the contribution of this term is usually much smaller than that of the differential extinction term $(\mathbf{1} \times \mathbf{F} - \mathbf{F} \times \mathbf{1})$ because the latter is proportional to the first power of the polarizability, whereas the differential forward scattering term is proportional to the second power of the polarizability (see Eq. 13).

Now let us consider the differential extinction terms in M_{14} and M_{41}. Even nonabsorbing objects that are chiral with dimensions close to the wavelength of light can extinguish the two incident circular polarizations differently due to preferential scattering. This differential scattering away from the main beam contributes in transmission to the circular dichroism of the sample. As seen above, this effect cannot be described in first Born approximation (this is related to the fact that the first Born approximation violates the conservation of energy) because, for nonabsorbing objects whose groups do not interact, the waves scattered by each group in the forward direction are always in phase with the incident wave; in this case there can be no interference between transmitted and scattered waves, regardless of the geometrical relationship among the polarizable groups, and the differential extinction effects vanish.

On the other hand, if interactions among groups are allowed, the geometrical arrangement of the neighboring groups causes a phase difference between the incident wave and the waves scattered in the forward direction (interference). If the polarizable groups are arranged chirally, the phase relationships will be different for right and left circular incident polarizations giving rise to differential extinction effects in M_{14} and M_{41}.

The differential extinction term of the bright field M_{14} Mueller matrix element in the second Born approximation is proportional to (see Eq. 13):

$$(\mathbf{1} \times \mathbf{F}_{2nd}^{\dagger} - \mathbf{F}_{2nd} \times \mathbf{1})_{\alpha\beta\gamma}\,(1 - \hat{\mathbf{z}}\hat{\mathbf{z}})_{\alpha\gamma}\,\hat{\mathbf{z}}_{\beta},$$

where $\mathbf{F}_{2nd}$ is:

$$\mathbf{F}_{2nd} \equiv \sum_{i}^{N} K_i\boldsymbol{\alpha}_i \cdot \left(\mathbf{1} + 4\pi k^2 \sum_{j \neq i} \Gamma_{ij} \cdot \alpha_j \cdot e^{i\mathbf{k}_o \cdot \mathbf{r}_{ij}}\right).$$

Using the last definition the differential extinction term of M_{14} can be expanded as:

$$\begin{aligned}
&(\mathbf{1} \times \mathbf{F}_{2nd}^{\dagger} - \mathbf{F}_{2nd} \times \mathbf{1})_{\alpha\beta\gamma}\,(1 - \hat{\mathbf{z}}\hat{\mathbf{z}})_{\alpha\gamma}\,\hat{\mathbf{z}}_{\beta} \\
&= \Bigg[\mathbf{1} \times \sum_{i}^{N} K_i\alpha_i^*\hat{\mathbf{t}}_i\hat{\mathbf{t}}_i - \sum_{i}^{N} K_i\alpha_i\hat{\mathbf{t}}_i\hat{\mathbf{t}}_i \times \mathbf{1} \\
&+ \mathbf{1} \times 4\pi k^2 \sum_{i}^{N}\sum_{j \neq i}^{N} K_i\alpha_i^*\alpha_j^*(\hat{\mathbf{t}}_j \cdot \Gamma_{ji}^* \cdot \hat{\mathbf{t}}_i)e^{-i\mathbf{k}_o \cdot \mathbf{r}_{ij}}\hat{\mathbf{t}}_j\hat{\mathbf{t}}_i \\
&- 4\pi k^2 \sum_{i}^{N}\sum_{j \neq i}^{N} K_i\alpha_i\alpha_j(\hat{\mathbf{t}}_i \cdot \Gamma_{ij} \cdot \hat{\mathbf{t}}_j)e^{i\mathbf{k}_o \cdot \mathbf{r}_{ij}}\hat{\mathbf{t}}_i\hat{\mathbf{t}}_j \times \mathbf{1}\Bigg]_{\alpha\beta\gamma} \\
&\cdot (1 - \hat{\mathbf{z}}\hat{\mathbf{z}})_{\alpha\gamma}\,\hat{\mathbf{z}}_{\beta}.
\end{aligned}$$

The first two terms correspond to the differential extinction in the first Born approximation and vanish when the individual polarizability tensors are symmectric and real. The last two terms are due to the interactions among groups. Expanding these two terms, we obtain

$$4\pi k^2 \sum_{i}^{N} \sum_{j\neq i}^{N} K_i\alpha_i\alpha_j [e^{-ik_o\cdot r_{ij}}(\hat{t}_j \cdot \Gamma_{ji}^* \cdot \hat{t}_i) + e^{ik_o\cdot r_{ij}}(\hat{t}_i \cdot \Gamma_{ij} \cdot \hat{t}_j)] \times [(\hat{t}_i \cdot \hat{\epsilon}_H)(\hat{\epsilon}_H \times \hat{t}_j) \cdot \hat{z} + (\hat{t}_i \cdot \hat{\epsilon}_V)(\hat{\epsilon}_V \times \hat{t}_j) \cdot \hat{z}],$$

where we have assumed that the polarizability tensors of the individual groups are symmetric and real, and we have used the relation $\mathbf{1} - \hat{z}\hat{z} = \hat{\epsilon}_H\hat{\epsilon}_H + \hat{\epsilon}_V\hat{\epsilon}_V$. The above expression does not vanish because of the complex phase factors introduced by group interactions and contained in the Γ-tensor.

As will be discussed in detail in the following paper, it is possible to separate theoretically and, under certain conditions also experimentally, the differential absorption (CD) and differential scattering (CIDS) contributions contained in the differential extinction term.

III B. Dark field M_{14} images of isotropic groups arranged in a chiral fashion

In section II B, it was mentioned that the dark field M_{i4} and M_{4i} (i = 1, 2, 3) images of a collection of nonabsorbing isotropic groups vanish in the first Born approximation. In higher Born approximations, however, this is no longer true (2–4). This will be shown analytically here as applied to imaging, using M_{14} as an example.

In the first Born approximation, the dark field M_{14} image is (See Eq. 21a of paper I [1]):

$$M_{14} = -iA \sum_{i}^{N} \sum_{j}^{N} K_iK_j e^{-i\Delta k'\cdot r_{ij}} (\alpha_i \times \alpha_j^{\dagger})_{\alpha\beta\gamma}(1 - \hat{z}\hat{z})_{\alpha\gamma}\hat{k}_{o\beta}, \quad (15)$$

where $A = 1/2I_o\ c/8\pi\ |D''|^2$, I_o is the intensity of the incident light, and we have made the usual $\hat{r} \approx \hat{z}$ approximation. When the polarizable groups are arranged in a chiral fashion, the quantity $(\alpha_i \times \alpha_j^{\dagger})_{\alpha\beta\gamma}(1 - \hat{z}\hat{z})_{\alpha\gamma}\hat{k}_o$ accounts for the circular intensity differential scattering (CIDS) of the object. To see this clearly, let us consider the dark field M_{14} image of two uniaxial groups with polarizabilities $\alpha_1 = \alpha_1\hat{t}_1\hat{t}_1$ and $\alpha_2 = \alpha_2\hat{t}_2\hat{t}_2$:

$$M_{14} \propto -i \sum_{i}^{N} \sum_{j}^{N} e^{i-\Delta k'\cdot r_{ij}} (\alpha_i \times \alpha_j^{\dagger})_{\alpha\beta\gamma}(1 - \hat{z}\hat{z})_{\alpha\gamma}\hat{k}_{o\beta}$$

$$= 2\sin(\Delta k' \cdot r_{12})\ \alpha_1\alpha_2\ [(\hat{t}_2 \times \hat{t}_1) \cdot \hat{k}_o][\hat{t}_2 \cdot \hat{t}_1 - (\hat{t}_2 \cdot \hat{z})(\hat{z} \cdot \hat{t}_1)].$$

If $\hat{t}_1$ and $\hat{t}_2$ are parallel or perpendicular to each other, and both $\hat{t}_1$ and $\hat{t}_2$ are perpendicular to $\hat{k}_o$, the quantity $(\hat{t}_2 \times \hat{t}_1) \cdot \hat{k}_o$ in the above equation becomes zero. Only when those uniaxial groups bear a chiral relationship, the quantity $(\hat{t}_2 \times \hat{t}_1) \cdot \hat{k}$ is not zero. Thus, the chiral relationship between the scattering groups is described by the quantity $\Sigma_i^N \Sigma_j^N (\alpha_i \times \alpha_j^{\dagger})_{\alpha\beta\gamma}(1 - \hat{z}\hat{z})_{\alpha\gamma}\hat{k}_{o\beta}$. However, when the polarizabilities of the scattering groups are isotropic, the CIDS is zero in the first Born approximation even if the groups bear a chiral relationship to each other. This can be seen by choosing two isotropic polarizabilities, $\alpha_1 = \alpha_1\mathbf{1}$ and $\alpha_2 = \alpha_2\mathbf{1}$, then:

$$M_{14} \propto \alpha_1\alpha_2\ (\mathbf{1} \times \mathbf{1})_{\alpha\beta\gamma}(1 - \hat{z}\hat{z})_{\alpha\gamma}\hat{k}_{o\beta} = -\alpha_1\alpha_2(\hat{z} \times \hat{z}) \cdot \hat{k}_o = 0.$$

When using higher Born approximations for the internal field, however, the dark field M_{14} image of an object consisting of transparent isotropic groups arranged in chiral fashion no longer vanishes. This can be understood in terms of the *anisotropy* induced in the polarizability of each group by its coupling to the other groups in the molecule. This induced anisotropy is the result of the interaction terms containing the tensor Γ_{ij}. For example, substituting the polarizability tensors α_i and α_j in Eq. 15 with the effective polarizabilities given by the expression inside the square brackets in Eq. 5, M_{14} becomes, in the second Born approximation:

$$M_{14} = -iA \sum_{i}^{N} \sum_{k}^{N} K_iK_k e^{-i\Delta k'\cdot r_{ik}} \Bigg[(\alpha_i \times \alpha_k^{\dagger}) + 4\pi k \Bigg[\sum_{l\neq k}^{N} e^{-ik_o\cdot r_{kl}} \alpha_i \times (\alpha_l^{\dagger} \cdot \Gamma_{lk}^* \cdot \alpha_k^{\dagger}) + \sum_{j\neq i}^{N} e^{ik_o\cdot r_{ij}} (\alpha_i \cdot \Gamma_{ij} \cdot \alpha_j) \times \alpha_k \Bigg] + (4\pi k^2)^2 \sum_{j\neq i}^{N} \sum_{l\neq k}^{N} e^{ik_o\cdot(r_{ij}-r_{kl})} (\alpha_i \cdot \Gamma_{ij} \cdot \alpha_j) \times (\dagger_l \cdot \Gamma_{lk}^* \cdot \dagger_k) \Bigg]_{\alpha\beta\gamma}(1 - \hat{z}\hat{z})_{\alpha\gamma}\hat{k}_{o\beta}.$$

In the above equation, the first term, proportional to $(\alpha_i \times \alpha_k^{+})_{\alpha\beta\gamma}\ (\mathbf{1} - \hat{z}\hat{z})_{\alpha\gamma}\hat{k}_{o\beta}$, corresponds to M_{14} in the first Born approximation and vanishes when the individual polarizability tensors are isotropic. The remaining three terms result from the interaction among groups and do not vanish even when the groups are spherically symmetric. This is because a diadic $\alpha_i \cdot \Gamma_{ij} \cdot \alpha_j$ is just equal to $\alpha_i\alpha_j\Gamma_{ij}$ when α_i and α_j are isotropic, and Γ_{ij} has, in general, complex off-diagonal elements.

This result is shown in Fig. 1, where we have generated the dark field M_{14} images of left- and right-handed helices consisting of 30 isotropic scattering groups. The radius and the pitch of the helices are 5 and 10 λ, respectively. Each helix has three complete turns. The axis of each helix coincides with the *y*-axis of the laboratory frame and the incident light propagates along this axis from the negative to the positive direction (see

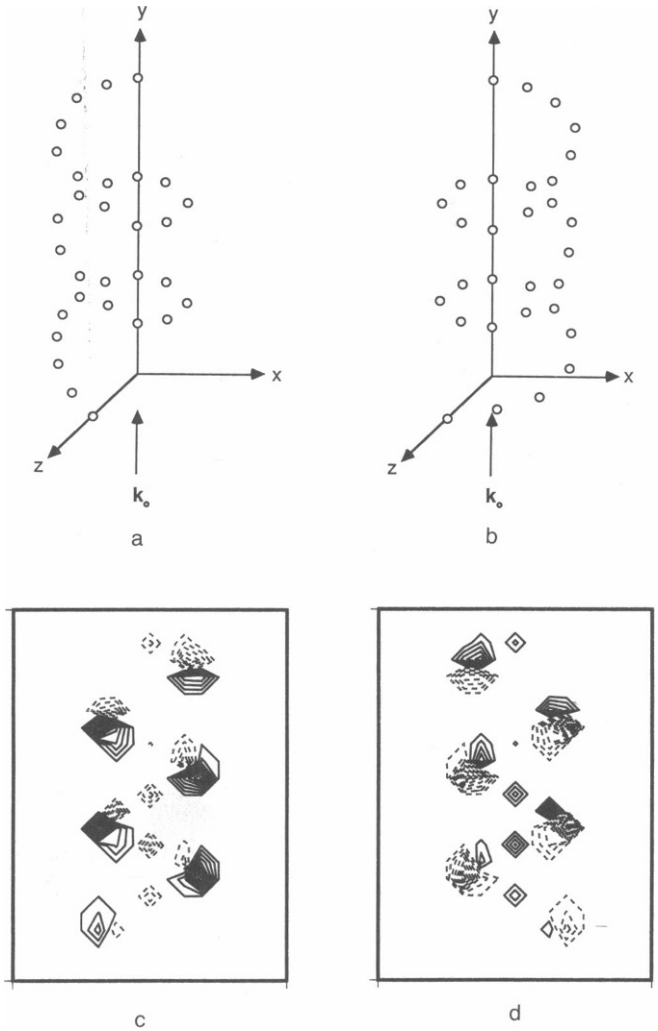

FIGURE 1 Left- (*a*) and right-handed (*b*) helices composed of 30 isotropic scattering groups (10 groups per turn) and their dark field M_{14} images (*c*, *d*), respectively. The radius and the pitch of the helices are 5 and 10λ, respectively. The incident light propagates along the *y*-axis from the negative to the positive direction. The light scattered in the *z* direction is captured by a lens to give a dark field image. For the computation of *c* and *d*, a resolution length of 1.22λ was used. Solid lines indicate positive CIDS values and short dashed lines indicate negative CIDS.

Fig. 1, *a* and *b*). The lens and the imaging screen are arranged such that the main contribution to the image is provided by light scattered at 90°. In this calculation, we have used an imaging system with a resolution length of 1.22 λ. Fig. 1, *c* and *d*, depict the CIDS images of these helices due to the anisotropy induced in the isotropic scattering groups by their mutual interactions. Notice the change of sign for the images of opposite handedness.

Finally, a word of caution about the interpretation of dark-field M_{14} (CIDS) images obtained through a differential polarization microscope. Tian and McClain (8) have shown that nonvanishing CIDS signals can be obtained from achiral oriented objects. It is not clear what the magnitudes of these signals relative to those associated with chiral structures of various dimensions and optical densities are, and therefore, it is difficult to make an estimate of their importance in common applications. It is unlikely, nonetheless, that such orientation effect could play an important role in but a few obvious cases. In Mueller images, the data is a spatial average of signals originated within an area of the size of the picture elements or "pixels" in the images. The pixel area is, roughly, of the order of the square of the resolution length of the microscope. Only in very specific and conspicuous cases do biological structures display uniaxiality extending to this long-range dimension (9). Therefore, nonchiral structures will usually not contribute to the magnitude and sign of the CIDS images.

IV. WHEN ARE HIGHER BORN APPROXIMATIONS REQUIRED?

The effects introduced in the Mueller matrix entries by group coupling have been illustrated in the previous sections, using the second and third Born approximations. This has been done for simplicity of the demonstrations and not to imply that incorporation of one or two additional orders suffices to estimate quantitatively the scattering and absorption cross-sections in all cases. Indeed, Keller and Bustamante (6, 10) have shown that certain optical activity effects such as the anomalous circular dichroism signals or "psi-type" CD, can only be explained using the all-order approach and the interaction matrix **A** (see Eq. 8 and following expressions). Furthermore, these authors found that the magnitude of the "psi-type" effects is dependent on the size of the chiral object, their shape and chromophore density. In particular, it was found that the effects are particularly pronounced for chiral objects of three-dimensional shapes and size commensurate to the wavelength of the light. Singham and Bohren (11) have recently analyzed the rate of convergence of the Born series in a variety of conditions. These authors have shown that the rate of convergence of the Born series depends on the number of dipoles used to describe the scattering particle, their shape, and their refractive index relative to the immersion medium. In the case of large three-dimensional objects with relative refractive indices of 1.3 or more, as many as 70 orders are required before convergence of the series is obtained.

An important question is then, when is the first Born approximation valid? In what follows, quantitative crite-

ria of the validity of the first Born approximation will be derived for a variety of optically anisotropic media.

In paper I (1), the two conditions for the validity of the first Born approximation (or Rayleigh-Gans approximation) were discussed. These are

$$|n - n'| \ll 1, kd|n - n'| \ll 1, \quad (16)$$

where d is the thickness of the optical medium, n is its complex refractive index, and n' is that of the surrounding medium. The first condition may be interpreted as the requirement that the incident wave not be appreciably reflected at the interface between the sample and the surrounding medium. The second condition, as the requirement that the phase or amplitude of the incident wave not be altered appreciably after the incident wave enters the sample. These criteria for optically thin samples are valid in regular scattering or absorption experiments. Differential polarization measurements, where the interactions between the medium and the two different polarizations are compared, require more stringent criteria.

To see this, we first analyze the case of an optically homogeneous medium, which can be thought as composed of very thin layers stacked in parallel. If light of well-defined initial polarization is incident perpendicularly to the outer face of the medium, conditions 16 only ensure minimal multiple reflections between successive layers. Inside an anisotropic medium there is an additional form of coupling between the layers due to the ability of the medium to modify the polarization of the incident light. As light travels through successive layers of the material its polarization is modified preserving a "memory" of the previous interaction. If this effect is substantial the next layer will experience largely modified incident polarizations. This form of *sequential coupling* among the layers of the material must be minimized to ensure that the optical medium is optically thin from a polarization stand point.

The need of additional criteria to account for the polarization of the light can be seen more clearly with the following example. A sample composed of a thin slab of calcite is sandwiched between two light flint glasses whose refractive index is 1.575 (the principal section and the optical axis of calcite are parallel to the interface between the light flint glass and the calcite). Calcite is a birefringent crystal which has refractive indices of 1.486 for the ordinary ray and 1.658 for the extraordinary ray. Now let us consider a linearly polarized incident wave whose electric field vector **E** is parallel to the principal section of calcite. Entering the calcite, the field **E** decomposes into two orthogonal components: one perpendicular to the optical axis of calcite and the other parallel to it. The components of **E** parallel and perpendicular to the optical axis propagate with the speeds of $c/1.486$ and $c/1.658$, respectively, where c is the speed of light in vacuum. The emergent wave which is a superimposed wave of the two orthogonal components is elliptically polarized due to the phase difference between them. Because the difference $|n - n'|$ between the flint glass and calcite is 0.003 (the mean refractive index of calcite is 1.572), this sample certainly satisfies the two conditions in Eq. 16, as long as 'kd' in Eq. 16 is small. However, the ellipticity of the emergent wave is large and determined by the difference between the two refractive indices and the thickness of calcite. Thus, it can be seen that criteria in Eq. 16 are not sufficient for the validity of the first Born approximation from a polarization stand point, and additional criteria to define an optically thin sample in differential polarization imaging are necessary.

These criteria will be derived in this section for three different kinds of media: (*a*) linearly anisotropic, (*b*) circularly anisotropic (optically active), and (*c*) linearly and circularly anisotropic (12). A linearly anisotropic medium displays linear dichroism (LD) and linear birefringence (LB); a circularly anisotropic medium displays circular dichroism (CD) and circular birefringence (CB).

IV A. Linearly anisotropic medium

Let us consider linearly polarized light traveling along the z-axis and incident on a linearly anisotropic medium of thickness d (see Fig. 2). The light is incident perpendicularly to one of the faces of the medium, placed at

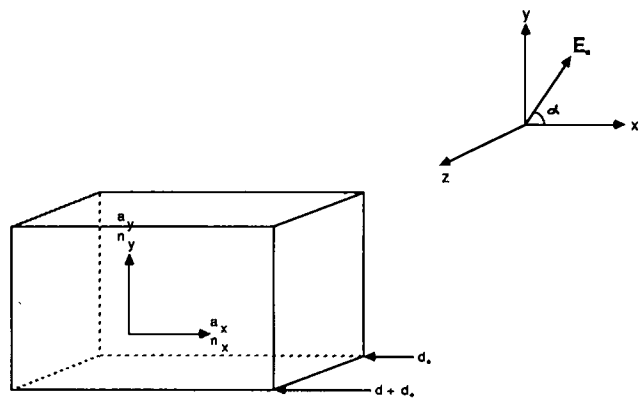

FIGURE 2 A slab of an optically thin linearly anisotropic sample. Its absorption coefficients and refractive indices along x and y directions are a_x, a_y, n_x, and n_y, respectively. Its thickness is d. This sample is illuminated by linearly polarized light whose plane of vibration makes an angle α with an x-axis.

position d_o along the direction of propagation z. If the plane of vibration of the electric field makes an angle α with the x-axis, we have:

$$\mathbf{E}_o = E_o e^{ikn_o d_o}(\cos\alpha\hat{\mathbf{x}} + \sin\alpha\,\hat{\mathbf{y}}), \tag{17}$$

where n_o is the refractive index of the surrounding medium, $\hat{\mathbf{x}}$ and $\hat{\mathbf{y}}$ are cartesian unit vectors and k is the wavenumber of the incident light. If we describe the absorption properties of this medium along x- and y-axes with molar absorption coefficients a_x and a_y, and the refractive properties with the refractive indices n_z and n_y, the transmitted electric field $\mathbf{E}_t$ is:

$$\mathbf{E}_t = E_o e^{ik(n_o d_o + nd)}\,(e^{-a_x cd/2}\,e^{ikd\Delta n_{x,y}}\cos\theta\,\hat{\mathbf{x}} + e^{-a_y cd/2}\,e^{-ikd\Delta n_{x,y}}\sin\theta\,\hat{\mathbf{y}}), \tag{18}$$

where

$$n \equiv \frac{n_x + n_y}{2}, \quad \Delta n_{x,y} \equiv \frac{n_x - n_y}{2}$$

and c is the concentration in moles/liter of the absorbing birefringent species. Note that the amplitudes along x- and y-axes are reduced by the amount of $e^{-a_x cd/2}$ and $e^{-a_y cd/2}$, respectively, and that the phase difference between the two orthogonal components is $2\Delta n_{x,y} kd$. Clearly, if $a_x = a_y \neq 0$ and $n_x = n_y$, that is, if the medium is isotropic, the polarization state of $\mathbf{E}_t$ will be the same as that of $\mathbf{E}_o$ and only the amplitude of $\mathbf{E}_t$ would be reduced by a factor of $e^{-acd/2}$, where $a \equiv a_x + a_y/2$. However, for a linearly anisotropic medium, $a_x \neq a_y$ and $n_x \neq n_y$ and the transmitted electric field $\mathbf{E}_t$ is in general elliptically polarized. Its ellipticity, inclination angle, and handedness are related to $(a_x - a_y)\,cd$ and $2\Delta n_{x,y} kd$. If $(a_x - a_y)\,cd$ is small, the major axis of the vibrating ellipse of the transmitted light will remain almost unaltered with respect to the direction of the vibration of the incident light. Therefore, the two quantities $(a_x - a_y)\,cd$ and $(n_x - n_y)\,kd$ must be small, if the polarization state of the transmitted light is to remain close to that of the incident light. Therefore, the amplitude and phase difference between the two orthogonal components of the transmitted fields must be much smaller than e and 2π, respectively. These conditions can be written as

$$|a_x - a_y|\,cd \ll 1 \quad \text{and} \quad |n_x - n_y|\,kd \ll 1. \tag{19}$$

IV B. Circularly anisotropic medium

Similarly, to obtain the conditions for an optically active medium whose absorptive properties for right and left circularly polarized light are described by the absorption coefficients a_R and a_L, and refractive properties by the refractive indices n_R and n_L, we decompose a linearly polarized incident light into right and left circularly polarized components.

$$\mathbf{E}_o = E_o e^{ikn_o d_o}\frac{1}{\sqrt{2}}(\hat{\boldsymbol{\epsilon}}_R e^{i\delta} + \hat{\boldsymbol{\epsilon}}_L e^{-i\delta})$$

$$= E_o e^{ikn_o d_o}(\hat{\mathbf{x}}\cos\delta - \hat{\mathbf{y}}\sin\delta), \tag{20}$$

where

$$\hat{\boldsymbol{\epsilon}}_R = \frac{1}{\sqrt{2}}(\hat{\mathbf{x}} + i\hat{\mathbf{y}}) \quad \text{and} \quad \hat{\boldsymbol{\epsilon}}_L = \frac{1}{\sqrt{2}}(\hat{\mathbf{x}} - i\hat{\mathbf{y}}).$$

When $\delta = 0$, $\mathbf{E}_o$ is a linearly polarized wave whose plane of polarization is along $\hat{\mathbf{x}}$; when $\delta > 0$ the plane of polarization is turned clockwise by an angle δ with respect to the $\hat{\mathbf{x}}$-axis. Then the transmitted electric field is written:

$$\mathbf{E}_t = \frac{E_o}{\sqrt{2}} e^{ik(n_o d_o + nd)}(e^{-a_R cd/2}\,e^{i(\delta + kd\Delta n_{R,L})}\hat{\boldsymbol{\epsilon}}_R + e^{-a_L cd/2}\,e^{-i(\delta + kd\Delta n_{R,L})}\hat{\boldsymbol{\epsilon}}_L),$$

where

$$n \equiv \frac{n_R + n_L}{2} \quad \text{and} \quad \Delta n_{R,L} \equiv \frac{n_R - n_L}{2}.$$

The difference between the amplitudes of the right and left circular components depends on $(a_R - a_L)cd$. And their phase difference which is the physical basis of optical rotation is $2\Delta n_{R,L} kd$. Thus, the two conditions,

$$|a_R - a_L|\,cd \ll 1 \quad \text{and} \quad |n_R - n_L|\,kd \ll 1, \tag{21}$$

must be satisfied by an optically active medium so that the change in polarization state of the internal field is not significant and for the effect of multiple interaction between the induced dipoles to be negligible.

IV C. Medium with mixed anisotropies

For a transparent medium displaying LB and CB, let us start with Maxwell equations for a dielectric medium in differential form.

$$\nabla \times \mathbf{E} = -\frac{1}{c}\dot{\mathbf{B}}, \quad \nabla \times \mathbf{H} = \frac{1}{c}\dot{\mathbf{D}},$$

where $\mathbf{E}$ is the electric vector, and $\mathbf{D}$ is the divergenceless electric displacement vector. $\mathbf{H}$ is the magnetic vector, and $\mathbf{B}$ is the magnetic induction. The "dot" denotes differentiation with respect to time. The above equations can be rewritten for periodical fields as:

$$n\hat{\mathbf{k}} \times \mathbf{E} = \mathbf{B}, \quad n\hat{\mathbf{k}} \times \mathbf{H} = -\mathbf{D}, \tag{22}$$

where n is the refractive index of the medium, and $\hat{\mathbf{k}}$ is the unit vector along which the electromagnetic field

propagates. We want to solve the above equations for n using the constitutive relations for a transparent medium displaying LB and CB. In this case four refractive indices will be found. The two positive roots are related to the velocities at which two orthogonal fields propagate in the direction of transmission. These fields are in general elliptical. Their eccentricity, handedness, and direction of major axis change from point to point along the line of propagation.

For a linearly anisotropic dielectric medium, the constitutive relations are:

$$\mathbf{D} = \boldsymbol{\epsilon}\mathbf{E}, \quad \mathbf{B} = \boldsymbol{\mu}\mathbf{H},$$

where $\boldsymbol{\epsilon}$ and $\boldsymbol{\mu}$ are the dielectric and magnetic permeability tensors, respectively. Here, we will assume that the medium is nonmagnetic so that $\boldsymbol{\mu} \approx 1$. In an optically active medium, there is a part of the electric displacement proportional to $\dot{\mathbf{H}}$ and a part of magnetic induction proportional to $\dot{\mathbf{E}}$. A molar parameter g is required to describe the optical activity of a macroscopic medium. The constitutive relations then become (13):

$$\mathbf{D} = \boldsymbol{\epsilon}\mathbf{E} - g\dot{\mathbf{H}}, \quad \mathbf{B} = \mathbf{H} + g\dot{\mathbf{E}}.$$

The above equations are again written as:

$$\begin{aligned} \mathbf{E} &= \boldsymbol{\epsilon}^{-1}\mathbf{D} + \boldsymbol{\epsilon}^{-1}gi\omega\mathbf{B} \\ \mathbf{H} &= \mathbf{B} - \boldsymbol{\epsilon}^{-1}gi\omega\mathbf{D}, \end{aligned} \tag{23}$$

where $\omega = 2\pi\nu$ is the angular frequency. Substituting Eq. 23 into Eq. 22, we obtain

$$\begin{aligned} n(\dot{\mathbf{k}} \times \boldsymbol{\epsilon}^{-1}\mathbf{D}) + in\omega g(\dot{\mathbf{k}} \times \boldsymbol{\epsilon}^{-1}\mathbf{B}) &= \mathbf{B} \\ n(\dot{\mathbf{k}} \times \mathbf{B}) - in\omega g(\dot{\mathbf{k}} \times \boldsymbol{\epsilon}^{-1}\mathbf{D}) &= \mathbf{D}. \end{aligned} \tag{24}$$

Now, taking $\hat{\mathbf{k}} = \hat{\mathbf{z}}$, Eq. 24 becomes

$$\begin{aligned} -n\frac{D_y}{\epsilon_y} - in\omega g\frac{B_y}{\epsilon_y} = B_x, \quad nB_y + in\omega g\frac{D_y}{\epsilon_y} = -D_x \\ n\frac{D_x}{\epsilon_x} + in\omega g\frac{B_x}{\epsilon_x} = B_y, \quad nB_x - in\omega g\frac{D_x}{\epsilon_x} = -D_y. \end{aligned} \tag{25}$$

Note that we have oriented the sample in such a way that the dielectric tensor $\boldsymbol{\epsilon}$ is diagonal.

$$= \begin{pmatrix} \epsilon_x & 0 & 0 \\ 0 & \epsilon_y & 0 \\ 0 & 0 & 0 \end{pmatrix}$$

If the medium is purely circularly anisotropic or if the light propagates along the optic axis of the medium, $\boldsymbol{\epsilon}$ would be a scalar quantity ($\epsilon_x = \epsilon_y$). Solving Eq. 25, we obtain

$$n^2 = \frac{\epsilon_x\epsilon_y[\bar{\epsilon} + 2(\omega g)^2 \pm \sqrt{\Delta\epsilon^2 + 8\bar{\epsilon}(\omega g)^2}]}{2[(\omega g)^2 - \epsilon_x][(\omega g)^2 - \epsilon_y]}, \tag{26}$$

where $\bar{\epsilon} \equiv \epsilon_x + \epsilon_y$ and $\Delta\epsilon \equiv \epsilon_x - \epsilon_y$. For small ωg, i.e., for small optical activities, this expression reduces to:

$$n^2 \approx \frac{\bar{\epsilon}}{2} \pm \left[\frac{\Delta\epsilon}{2} + \frac{2\bar{\epsilon}(\omega g)^2}{\Delta\epsilon}\right].$$

It can be seen that the above equation has two positive and two negative roots. The positive roots are

$$\begin{aligned} n_+ &= \sqrt{\epsilon_x}\left[1 + \frac{2\bar{\epsilon}(\omega g)^2}{\Delta\epsilon\epsilon_x}\right]^{1/2} \approx \sqrt{\epsilon_x}\left(1 + \frac{2\bar{\epsilon}(\omega g)^2}{\Delta\epsilon\epsilon_x}\right) \\ n_- &= \sqrt{\epsilon_y}\left[1 + \frac{2\bar{\epsilon}(\omega g)^2}{\Delta\epsilon\epsilon_y}\right]^{1/2} \approx \sqrt{\epsilon_y}\left(1 + \frac{2\bar{\epsilon}(\omega g)^2}{\Delta\epsilon\epsilon_y}\right). \end{aligned}$$

The difference between these refractive indices may be regarded as a measure of degree of change in the polarization state of the internal field with respect to that of the incident field. And that should be small in order for the first-Born approximation to be valid. This criterion can be then written:

$$|\Delta n| = |n_+ - n_-| = \left|(\sqrt{\epsilon_x} - \sqrt{\epsilon_y}) + \frac{\bar{\epsilon}(\omega g)^2}{\Delta\epsilon}\left(\frac{1}{\sqrt{\epsilon_x}} + \frac{1}{\sqrt{\epsilon_y}}\right)\right| \ll 1. \tag{27}$$

The above equation indicates that both LB (expressed as $\sqrt{\epsilon_x} - \sqrt{\epsilon_y}$ in Eq. 28) and CB (represented by the factor g) must be small to insure that the samples are optically thin. Note that, in this approximation, the terms related to LB and CB are independent of each other. Therefore, when one of the two anisotropic properties of the medium is not present ($g = 0$ for example), the contribution of the other one ($\sqrt{\epsilon_x} - \sqrt{\epsilon_y}$) remains.

V. OPTICAL SECTIONING IN DIFFERENTIAL POLARIZATION IMAGING OF OPTICALLY DENSE SAMPLES

V A. The effect of strong interaction between induced dipoles on optical sectioning

In the second paper of this series (12), it was shown that optical sectioning is possible in differential polarization imaging. If a sample is optically dense, however, it might be difficult to perform optical sectioning in differential polarization imaging because the layer which is in focus is affected by the fields induced by the neighboring layers inside the sample. An alternative way of describing this is that in optically thick samples the polarization state of the light is altered substantially as it propagates through the medium and the polarization of the field is not well defined for layers lying inside the sample. This effect is demonstrated by means of bright field M_{12}

images of a model system made up of two layers (planes) perpendicular to the optical axis of the imaging system. The geometry of the model system is shown in Fig. 3. A plane, referred to as the radial plane, see Fig. 3 *c*, where eight uniaxial groups are arranged in a radial fashion, is in focus. The other plane, referred to as the parallel plane has eight uniaxial groups arranged in parallel. This plane is situated behind the radial plane at a distance of 6.7λ which is larger than the setting accuracy of this imaging system (14). Fig. 4 *a* is the bright field M_{12} image of the radial plane alone and has a symmetrical pattern of clover-leaf with alternating signs. Fig. 4 *b* is the bright field M_{12} images of the sample described in Fig. 3 *a* and computed using the second Born approximation. As expected, the M_{12} image in Fig. 4 *b* is deformed compared with Fig. 4 *a*: the size of the vertical lobes has increased while the horizontal lobes are reduced. Thus, when the sample is optically dense and the interaction between these two planes is quite strong requiring higher Born approximations, the M_{12} image pattern of the radial plane which is in focus, is deformed by the influence of the adjacent parallel plane. In this case it

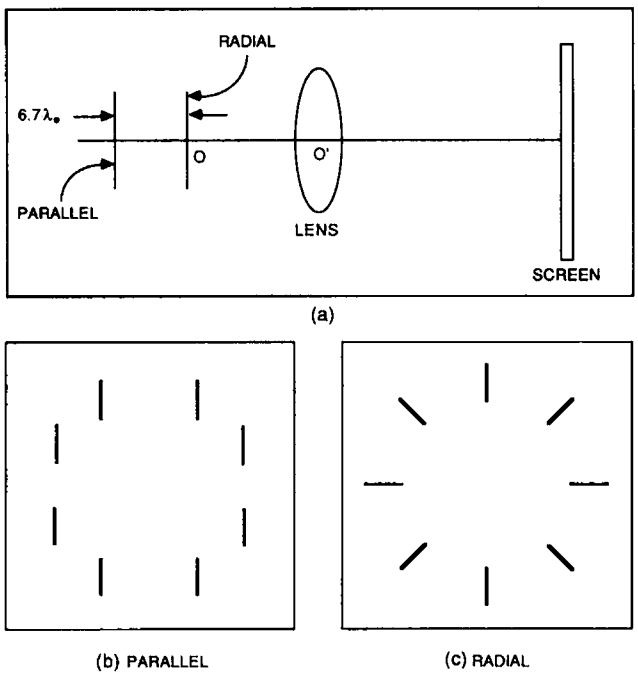

FIGURE 3 Geometry of the model used for the computation of the linear dichroism (M_{12}) images in bright field (*a*). This model represents a sample composed of one parallel and one radial plane (*b* and *c*). The radial plane is in focus, and contains eight absorbing uniaxial groups. The parallel plane contains eight absorbing uniaxial groups which are parallel to each other as shown in *b*. The diameter of these circular planes, the resolution length, and the magnification of the imaging system are 1.3, 2.2λ, and 1, respectively.

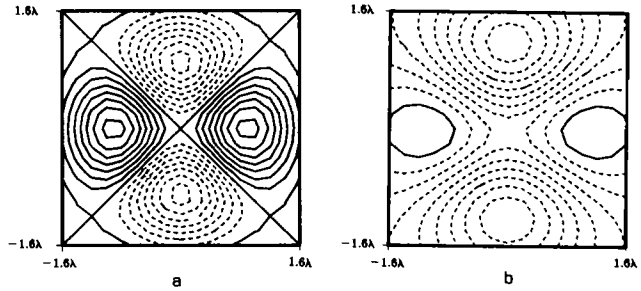

FIGURE 4 (*a*) The bright field M_{12} image of the radial plane shown in Fig. 3 *b*, calculated using the first Born approximation, (*b*) the bright field M_{12} image of a sample composed of both the parallel and the radial planes (Fig. 3), computed using the second Born approximation.

will not be easy to obtain the true differential polarization image of a certain layer in the sample. The net effect of the influence from neighboring layers inside the sample is to increase the depth of field of the imaging system. Consequently, to reduce the influence from the adjacent layers, setting accuracies higher than those used for optically thin samples will be required when studying optically dense specimens.

VI. SUMMARY AND CONCLUSIONS

The mathematical expressions of differential polarization images have been developed in this paper using higher Born approximations. These equations have the same form as those obtained in the first Born approximation. Except that the polarizability tensors used in the first Born approximations must be replaced in higher Born approximations by *effective polarizabilities,* which include the effects of mutual interactions among the groups. Some new features introduced into the differential polarization images by including these interactions are summarized below. (*a*) In the first Born approximation the *dark field* M_{i4} (i = 1, 2, 3) and their transposes always vanish for a collection of the isotropic polarizable groups. In higher Born approximations, however, these entries survive due to the anisotropy induced in each polarizable group by the coupling among groups inside the object. (*b*) When an object is composed of a collection of isotropic polarizable groups, the off-diagonal Mueller elements in *bright field* vanish in the first Born approximation. In higher Born approximations, none of the bright field Mueller images vanish if the isotropic groups bear the specific geometrical relationship to which each Mueller element is sensitive. (*c*) When using the first Born approximation, the *bright field* M_{14} and M_{41} images of a collection of real symmetric

polarizability tensors are always zero, even if the groups bear a chiral relationship to each other. Except for these two elements, none of the Mueller elements in this case are necessarily zero. In higher Born approximations, if the polarizable groups are arranged in a chiral fashion, M_{14} and M_{41} do not vanish. In this case, the nonvanishing M_{14} image results from the differential power loss of incident right and left circularly polarized light off the transmitted beam by the chiral object. In the case of M_{41}, it is due to the ability of the chiral object to introduce preferentially right and left circularity in the scattered light, when the incident light is unpolarized.

The quantitative criteria to determine when higher Born approximations are required in the description or interpretation of differential polarization images have been derived. These criteria define the limits to the thickness and the degree of anisotropy of an optically thin sample.

Finally, it has been shown that the effect of group coupling in the sample can affect substantially the ability to perform optical sectioning in differential polarization imaging.

This work was supported by grants from the National Science Foundation (grant #DIR-8820732), the National Institute of Health (grant #GM-32543), the Center for High Technology and Materials (UNM), the Minority Biomedical Research Support (grant #5-S06-RR0139-15), and the Student Research Allocation Committee of the Graduate Student Association (UNM).

Received for publication 25 July 1990 and in final form 17 December 1990.

REFERENCES

1. Kim, M., D. Keller, and C. Bustamante. 1987. Differential polarization imaging: I. Theory. *Biophys. J.* 52:911–927.
2. McClain, W. M., J. A. Schauerte, and R. A. Harris. 1984. Model calculations of intramolecular interference effects in Rayleigh scattering from solutions of macromolecules. *J. Chem. Phys.* 80:606–616.
3. Bustamante, C., M. F. Maestre, D. Keller, and I. Tinoco, Jr. 1984. Differential scattering (CIDS) of circularly polarized light by dense particles. *J. Chem. Phys.* 80:4817–4823.
4. Tinoco, I. Jr., W. Mickols, M. F. Maestre, and C. Bustamante. 1987. Absorption, scattering, and imaging of biomolecular structures with polarized light. *Annu. Rev. Biophys. Biophys. Chem.* 16:319–349.
5. Keller, D. 1984. Scattering optical activity of chiral molecules: circular intensity differential scattering and circular differential imaging. Ph.D. thesis. University of California, Berkeley, CA.
6. Keller, D., and C. Bustamante. 1986. Theory of the interaction of light with large inhomogeneous molecular aggregates. I. Absorption. *J. Chem. Phys.* 84:2961–2971.
7. Jackson, J. D. 1962. Classical Electrodynamics. John Wiley & Sons Inc., New York.
8. Tian, D., and W. M. McClain. 1989. Nondipole light scattering by partially oriented ensembles. III. The Muller pattern for achiral molecules. *J. Chem. Phys.* 91:4435–4439.
9. Finzi, L., C. Bustamante, G. Garab, and C. Juang. 1989. Direct observation of large chiral domains in chloroplast thylakoid membranes by differential polarization microscopy. *Proc. Natl. Acad. Sci. USA.* 86:8748–8752.
10. Keller, D., and C. Bustamante. 1986. Theory of the interaction of light with large inhomogeneous molecular aggregates. II. Psi-type circular dichroism. *J. Chem. Phys.* 84:2972–2980.
11. Singham, S. B., and C. F. Bohren. 1988. Light scattering by an arbitrary particle: the scattering-order formulation of the coupled-dipole method. *J. Opt. Soc. Am.* A5:1867–1871.
12. Kim, M., L. Ulibarri, and C. Bustamante. 1987. Differential polarization imaging. II. Symmetry properties and calculations. *Biophys. J.* 52:929–946.
13. Condon, E. U. 1937. Theories of optical rotatory power. *Rev. Mod. Phys.* 9:432–457.
14. Inoue, S. 1986. Video Microscopy. Plenum Publishing Corp., New York. 584 pp.